

## EXPANSION OF THE SUPERGRANULAR MAGNETIC NETWORK THROUGH THE SOLAR ATMOSPHERE

T. AIOUAZ

High Altitude Observatory, National Center for Atmospheric Research, P.O. Box 3000, Boulder, CO 80307; aiouaz@ucar.edu

AND

M. P. RAST

Laboratory for Atmospheric and Space Physics, Department of Astrophysical and Planetary Sciences, University of Colorado, Boulder, CO 80309-0391

*Received 2006 May 31; accepted 2006 July 6; published 2006 August 8*

### ABSTRACT

The solar magnetic field has its footpoints in the photosphere, extends through the chromosphere, and is thought to expand through the transition region and into the corona. It is organized by fluid motions to form strong flux concentrations within the boundaries of the supergranular convection cells. These boundaries are the network lanes observed in line emission, and they display increasing width with height through the solar atmosphere. The network field concentrations are surrounded by a mixed-polarity internetwork magnetic field on the scale of granulation. We use a potential magnetic field extrapolation of synthetic photospheric magnetograms to study the magnetic network topology and the effects of a mixed-polarity background field on the network expansion with height through the solar atmosphere. We find that the expansion of the network boundary with height deviates significantly from the funnel expansion model. Moreover, we find that the background magnetic field has a considerable effect on the filling factor of the network area with height, even though the background flux is strictly equal to zero.

*Subject headings:* Sun: atmosphere — Sun: chromosphere — Sun: magnetic fields

*Online material:* color figure

### 1. INTRODUCTION

The magnetic field in the solar atmosphere originates in magnetic elements in the photosphere. Plasma flows in the photospheric layers carry the magnetic field to the edges of the supergranular convection cells, resulting in a larger magnetic flux in the cell boundaries than in their interiors. The upward extension of these boundaries is observed as network lanes, which are bright in chromospheric emission with increasing contrast to height, showing contrast ratios of nearly an order of magnitude in the extreme-ultraviolet (Reeves 1976). It is believed that the network magnetic field provides the basic channel for energy transport and heating of the solar chromosphere and corona and for the acceleration of the solar wind (e.g., Reeves 1976; Gabriel 1976; Marsch & Tu 1997; Vocks & Mann 2003; Aiouaz et al. 2005). Knowledge of the geometric expansion of the network with height can provide constraints on the energy budget of the solar atmosphere.

To date, theoretical modeling of a single flux tube's cross section with height (e.g., Gabriel 1976; Hackenberg et al. 2000) has largely provided us with the interpretive background to direct observations of network expansion (e.g., Patsourakos et al. 1999). Only recently has attention been given to the role of the internetwork field in determining the geometric properties of the field with height (Schrijver & Title 2003). This Letter examines the three-dimensional structure of the network magnetic field resulting from an imposed synthetic photospheric boundary flux. It focuses on the effects of the magnetic variations within the network and the presence of small-scale internetwork elements on the network expansion through the solar atmosphere.

### 2. SYNTHETIC MAGNETOGRAMS

Supergranular cells are distributed fairly uniformly over the solar disk with a horizontal scale of approximately 20–30 Mm. Here we tile a horizontal plane periodically with hexagonal cells

20 Mm in diameter and surrounded by 2 Mm-wide lanes. The network lanes (delineated with long dashed lines in Fig. 1) are the seed areas for a random distribution of strong network magnetic field concentrations.

We create three different magnetic field topologies of increasing complexity by specifying the vertical magnetic field on the lower boundary of the domain (Fig. 1). In the first case, 100 unipolar magnetic field concentrations are randomly distributed within the network lanes (left panel in Fig. 1); in the second case, concentrations of mixed polarity (150 positive and 50 negative) are randomly placed within the network (middle panel in Fig. 1). In these cases, no magnetic field concentrations are placed within the supergranular cells. The flux concentrations are Gaussian-shaped with a full-width at half-maximum (FWHM) equal to 1 Mm and of unit ( $\pm 1$ ) amplitude. The final case (right panel in Fig. 1) is similar to the second, with mixed polarities within the network lanes (again 150 positive and 50 negative), but with an additional background field component added. This background field consists of 500 weak magnetic field concentrations of mixed polarity (FWHM equal to 0.5 Mm and amplitudes of  $\pm 0.1$ ) randomly distributed within the cells. Care is taken to keep the total flux of the internetwork background field equal to zero, while the net flux of the network field is nearly the same (minor differences due to overlap of the Gaussian profiles) in all three cases.

### 3. THE NETWORK EXPANSION MODEL

At present, we have to rely on field extrapolation methods to infer properties of the coronal field. Simple fields, such as potential magnetic fields, are broadly applicable and still widely invoked in the literature. Even though this is an extreme oversimplification, neglecting currents, flows, and radiative transfer in the solar photosphere, it allows us to study the atmospheric magnetic topology resulting from a given boundary flux.

To determine the magnetostatic potential field, we solve the

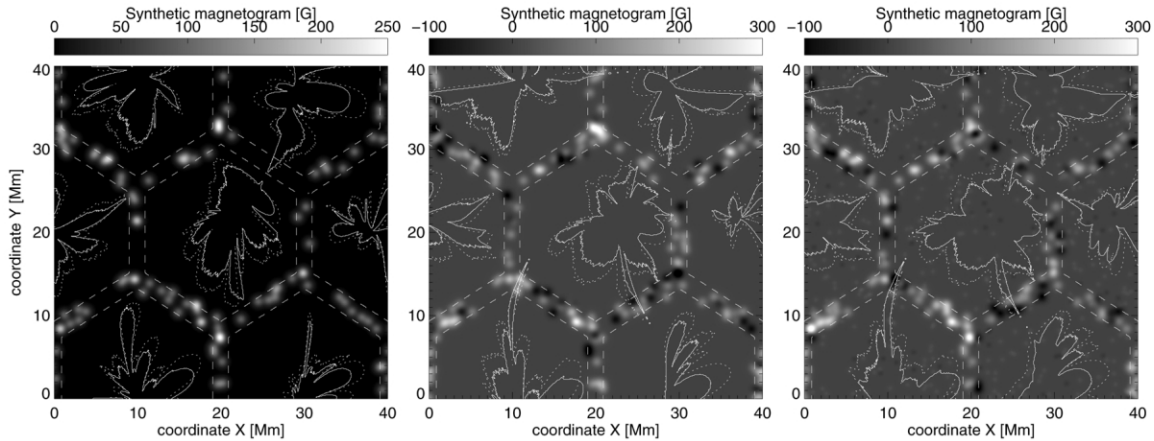


FIG. 1.—Synthetic magnetograms with three different magnetic topologies. *Left*: Unipolar magnetic field concentrations within the network area. *Middle*: Mixed-polarity magnetic field concentrations within the network area. *Right*: Mixed-polarity magnetic field concentrations within the network area, with additional mixed-polarity internetwork background field. The long-dashed lines delineate the seed area for the strong network magnetic field concentrations, assumed to be the network area. The gray scale indicates the magnetic field strength. The solid and dashed lines are contours of the network mask calculated from the network expansion model at heights  $z = 3$  Mm and  $z = 10$  Mm, respectively.

linear equation,  $\nabla \times \mathbf{B} = 0$ , in the Fourier domain (see Alisandrakis 1981). The potential magnetic field solution is fully determined by the values imposed at the lower boundary (the vertical field given by the synthetic magnetograms described in § 2), an assumed horizontal periodicity, and an upper boundary condition, which we take to be vertical field at infinity.

Once all three components of the magnetic field are computed, we are able to follow the expansion of the network. At any chosen height, for each pixel of the map we trace back the corresponding magnetic field line to the photospheric plane. We define as network any pixel whose magnetic field traces back to the network seed area of the magnetogram (within the long-dashed boundaries in Fig. 1). We thus obtain a network mask at each height and can follow the expansion of these regions through the atmosphere. We indicate the shape of the network mask for each synthetic magnetograms at heights  $z = 3$  Mm and  $z = 10$  Mm with solid and dashed curves, respectively, in Figure 1.

The lower left panel in Figure 2 shows the variation of the network filling factor (network area over the total field of view) with height in the atmosphere. The result from case I (unipolar network) is shown with a dotted curve, that of case II (mixed-polarity network) is plotted with a long-dashed curve, and case III's (mixed-polarity network plus internetwork field) is shown using a solid curve. In addition, we use the two-dimensional magnetic funnel model as defined by Hackenberg et al. (2000) to calculate the variation of the filling factor with height implied by a single magnetic funnel. Hackenberg et al. (2000) modeled supergranulation in two dimensions by imposing along the lower boundary a compact vertical field surrounded by an oppositely signed, more diffused return field of lower flux. We similarly define an axisymmetric funnel of radius  $L/2$  and total net flux  $\phi_{\text{net}}$ . The high degree of symmetry assumed by the Hackenberg et al. (2000) model yields a current-free (also called potential) magnetic field solution within the domain. We calculate the filling factor at each height by defining the funnel area as that of a disk whose radius is the distance from the funnel center to the last open magnetic field line. The variation of the funnel filling factor with height is plotted with a dashed curve (lower left panel in Fig. 2), where the horizontal length scale of the funnel  $L$  was normalized so that its filling factor is equal to that of cases I and II at  $z = 10$  Mm.

#### 4. RESULTS AND DISCUSSIONS

The lower left panel in Figure 2 displays clearly that after a height of  $z \approx 3$  Mm, the network expansion in the unipolar case (case I, *dotted curve*) and the case of mixed polarities (case II, *long-dashed curve*) become nearly indistinguishable. Since mixed polarities within the network in the later case imply the presence of loops within the network itself, this result demonstrates that these loops influence the network expansion at heights lower than  $z \approx 3$  Mm only. Since the network net flux in these two cases is equal, the filling factors at greater heights converge.

In contrast, the results from case III show that the presence of a weak background field significantly alters the network filling factor throughout the domain. The presence of the internetwork field significantly reduces the expansion of the network, even in the uppermost layers (10% less network at 10 Mm). Since care was taken to keep the total flux of the internetwork background zero, this continued suppression of the network area with height reflects the presence of a randomly seeded weak field adjacent to the network lanes. The weak field concentrations, by providing low-lying loop footpoints with one footpoint within the network and the other without (see right panels in Fig. 2), prevent some of the network field from reaching the upper boundary of the domain. The background magnetic field thus acts to redistribute the network flux into the internetwork region, allowing some of the internetwork field to remain open at the upper boundary.

Finally, the results from all three potential field extrapolations are significantly different than that expected based on the expansion of the magnetic funnel model (Fig. 2, *dashed line*). The network expansion calculated from the three-dimensional extrapolation of synthetic magnetograms composed of many magnetic field concentrations deviates significantly from the expansion of the single magnetic funnel at almost all heights. Nevertheless, it is possible to approximate the variation of the network filling factor resulting from any of the three synthetic magnetograms using a combination of two-dimensional axisymmetric magnetic funnels. The values of the net flux ( $\phi_{\text{net}}$ ) and horizontal length scale ( $L$ ) of each funnel would have to be determined so that the combination approximates the filling factor resulting from the synthetic magnetograms (see sketch in the top left panel in Fig. 2).

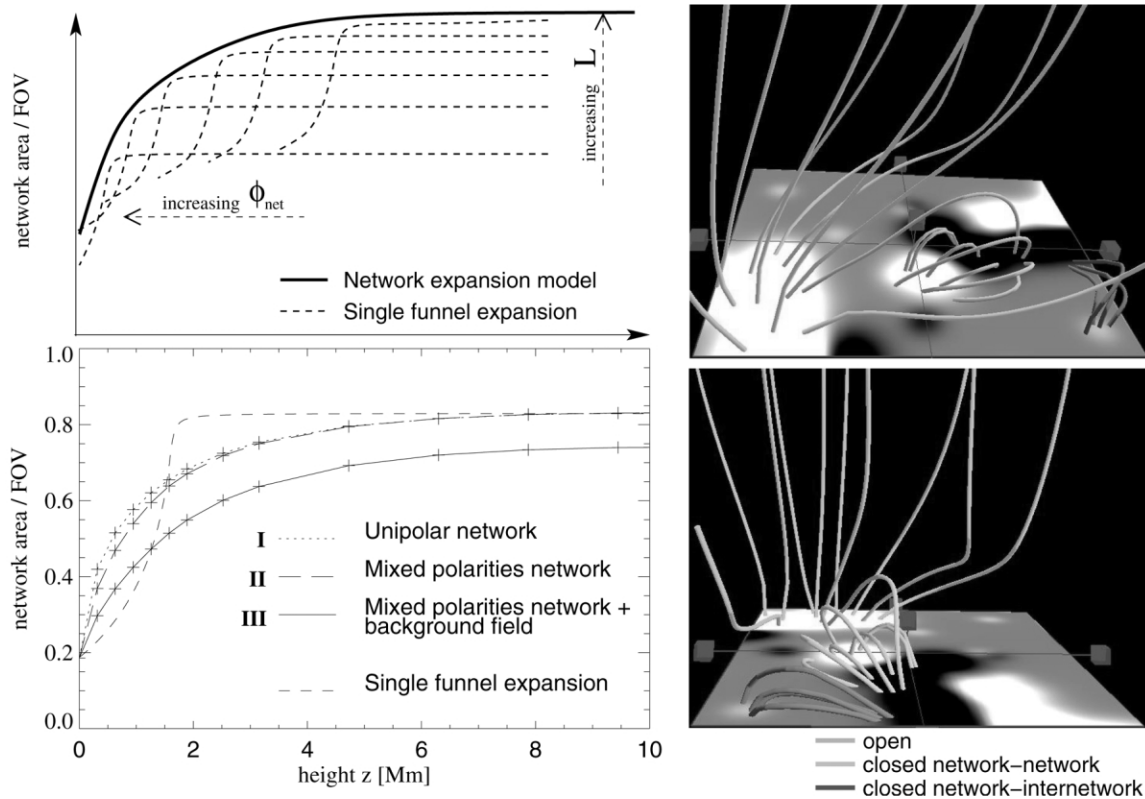


FIG. 2.—*Lower left panel:* Network filling factor (area of network/field of view [FOV]) as a function of height in the atmosphere. Case I is plotted with a dotted curve, case II with a long-dashed curve, and case III with a solid curve. The funnel expansion profile is shown with a dashed curve. The upper left panel is a sketch and illustrates how a combination of various funnel expansions can fit the variation of the network filling factor with height. The dashed arrows indicate the dependency of the funnel expansion profile variation on the net magnetic flux ( $\phi_{\text{net}}$ ) and the horizontal length scale ( $L$ ). The right panels show a sample of magnetic lines calculated in case III from a front and left point of view (*upper and lower panels, respectively*; images from the VAPoR visualization software; Clyne & Rast 2005). [See the electronic edition of the Journal for a color version of this figure.]

## 5. CONCLUSIONS

The main goal of this Letter was to calculate the network filling factor variation with height using synthetic magnetograms of increasing complexity. The result demonstrates that the effect of loops within the network area are rather low-lying. This is of significant importance because it places stringent constraints on observations aimed at studying the magnetic network topology. Furthermore, the presence of small loops, with one footpoint within the network and the other without, greatly affects the network filling factor to significant heights, even though the background internetwork flux is strictly equal to zero. This result demonstrates the importance of the unresolved small-scale internetwork magnetic field on the configuration of the network at chromospheric and coronal heights. Finally, the magnetic funnel model, derived from the well-

known Gabriel (1976) model, has been used as a reference model for observations of the expansion of the network through the atmosphere. This should be reconsidered in light of our results, and multiple funnel models, more realistic field extrapolations, or magnetohydrodynamic models should be considered for future comparison with observations.

This study motivates further work on network magnetic field topology and has implications for our understanding of the chromospheric and coronal field configuration above the quiet Sun.

We would like to thank Thomas Holzer for his helpful comments and discussions and for his careful reading of the manuscript.

## REFERENCES

- Aiouaz, T., Peter, H., & Keppens, R. 2005, *A&A*, 442, L35  
 Alissandrakis, C. E. 1981, *A&A*, 100, 197  
 Clyne, J., & Rast, M. 2005, *Proc. SPIE*, 5669, 284  
 Gabriel, A. H. 1976, *Philos. Trans. R. Soc. London A*, 281, 339  
 Hackenberg, P., Marsch, E., & Mann, G. 2000, *A&A*, 360, 1139  
 Marsch, E., & Tu, C.-Y. 1997, *Sol. Phys.*, 176, 87  
 Patsourakos, S., Vial, J.-C., Gabriel, A. H., & Bellamine, N. 1999, *ApJ*, 522, 540  
 Reeves, E. 1976, *Sol. Phys.*, 46, 53  
 Schrijver, C. J., & Title, A. M. 2003, *ApJ*, 597, L165  
 Vocks, C., & Mann, G. 2003, *ApJ*, 593, 1134